Polarized electromagnetic radiation from spatially correlated sources

Abhishek Agarwal,* Pankaj Jain,† and Jagdish Rai
Physics Department, Indian Institute of Technology, Kanpur 208016, India
(Received 10 March 2000; revised manuscript received 10 May 2001; published 19 November 2001)

We consider the effect of spatial correlations in sources of polarized electromagnetic radiation. We evaluate the coherency matrix for a spatially extended three-dimensional source in order to obtain its dependence on the angular position of the observer in the far zone. We find a general condition on the source correlation matrix under which the polarization in the far zone shows no angular dependence. In general, however, we find that the polarization shows a rather striking dependence on the direction of observation. We illustrate this effect by considering some examples of monochromatic spatially correlated sources. The sources, assumed to be monochromatic, are constructed out of dipoles aligned along a line such that their orientation is correlated with their position. In one representative example, the dipole orientations are prescribed by a generalized form of the standard von Mises distribution for angular variables such that the azimuthal angle of dipoles is correlated with their position. In another example the tip of the dipole vector traces a helix around the symmetry axis of the source. Possible experimental observation of this effect, by considering an analog of the standard two-slit interference experiment, is also discussed. The effect may find useful applications in certain astrophysical sources.

DOI: 10.1103/PhysRevE.64.066605 PACS number(s): 41.90.+e,42.50.Ar

I. INTRODUCTION

In a series of interesting papers Wolf [1–3] studied the spectrum of light from spatially correlated sources and found, remarkably, that in general the spectrum does not remain invariant under propagation even through vacuum. The phenomenon was later confirmed experimentally [4–6] and has been a subject of considerable interest [7]. Further investigations of the source correlation effects have been done in the time domain theoretically [8] and experimentally [9]. Several applications of the effect have also been proposed [10–14]. In a related development it has been pointed out that spectral changes also arise due to static [15–19] and dynamic scattering [20–24]. The Wolf effect arises due to coherence between spatially separated sources. The effect goes away if the degree of spectral coherence satisfies a scaling law derived in Ref. [1]. Furthermore, the spectrum in the far zone also depends on the direction of observation, if the degree of spectral coherence $\mu(k\hat{\mathbf{R}},\omega)$, where $\hat{\mathbf{R}}$ is a unit vector in the direction of observation and $\omega(=kc)$ is the frequency, is not independent of $\hat{\mathbf{R}}$.

In the present paper we investigate polarization properties of spatially correlated sources. This has recently been a subject of considerable interest [25–31]. In a recent paper we studied the spectral dependence of polarization from such sources [32]. In that paper we showed that in the far zone polarization from such sources shows spectral dependence unless the source correlation matrix satisfies a scaling law analogous to the scaling law found by Wolf in his analysis of spectral shifts due to spatial correlations. In the current paper we are interested in the angular dependence of the polarization due to interference between the waves emitted from different points on a spatially extended source. In analogy with the observed spectral shifts, we expect nontrivial polarization effects if the light emitted from spatially correlated sources is polarized.

II. ANGULAR AND SPECTRAL DEPENDENCE OF CORRELATION MATRIX

We first briefly review the results of Ref. [32]. We consider a spatially extended source which is described by the charge density $\rho^{(r)}(\mathbf{r},t)$ and current density $\mathbf{J}^{(r)}(\mathbf{r},t)$. We evaluate the electric field due to this source at the point Q (Fig. 1) in the far zone. Let $\mathbf{E}(\mathbf{R},\omega)$ and $\mathbf{J}(\mathbf{r},\omega)$ be the analytic signals associated with the Fourier transform of the electric field and the current density, respectively. Here $\mathbf{R}$ is the position vector of the observation point Q, $\mathbf{r}$ the position vector of any point P on the source, and ω is the frequency. In the far zone, $\mathbf{E}(\mathbf{R},\omega)$ is given by [32]

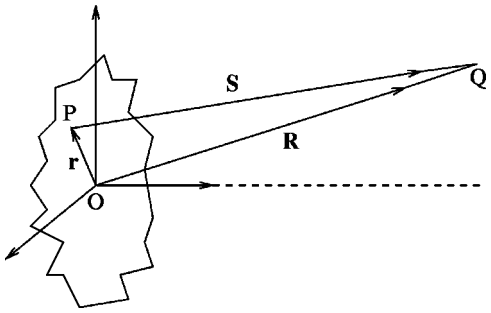

FIG. 1. Schematic illustration of spatially extended three-dimensional (3D) source of polarized radiation and the observation point Q located at position vector $\mathbf{R}$ from the source. P represents any point on the source located at position vector $\mathbf{r}$ with respect to the origin O of the coordinate system and at a distance $S=|\mathbf{S}|$ from Q.

*Present address: Physics Department, University of Rochester, Rochester, NY 14627.
†Email address: pkjain@iitk.ac.in

 ©2001 The American Physical Society

$$\mathbf{E}(\mathbf{R},\omega)=\frac{i\omega}{4\pi\epsilon_0 c^2}\int d^3r\frac{e^{i\omega S/c}}{R}[\mathbf{J}(\mathbf{r},\omega)-\mathbf{J}(\mathbf{r},\omega)\cdot\hat{\mathbf{R}}\hat{\mathbf{R}}], \tag{1}$$

where $\mathbf{S}=\mathbf{R}-\mathbf{r}$, $S=|\mathbf{S}|$, $\hat{\mathbf{R}}=\mathbf{R}/R$, and $R=|\mathbf{R}|$. The dimensions of the source are assumed to be much smaller than its distance to the observation point and hence higher orders in $1/R$ are dropped in obtaining this result.

The coherency matrix in the radiation zone is given by

$$J_{ij}(\mathbf{R},\omega)=Z(\omega)\sum_{l,m}\int d^3r_a d^3\Delta\frac{e^{ik\hat{\mathbf{R}}\cdot\mathbf{\Delta}}}{R^2}\xi_{il}W^S_{lm}(\mathbf{r}_a,\mathbf{\Delta},\omega)\xi_{mj}, \tag{2}$$

where $\mathbf{r}_a=(\mathbf{r}+\mathbf{r}')/2$, $\mathbf{\Delta}=\mathbf{r}'-\mathbf{r}$, $\mathbf{r}$ and $\mathbf{r}'$ are the position vectors of any two points located on the source, $Z(\omega)$ is an overall normalization factor which will not play any role in our analysis, $k=\omega/c$, $\xi_{ij}=-\hat{R}_i\hat{R}_j+\delta_{ij}$, and $W^S_{ij}(\mathbf{r}_a,\mathbf{\Delta},\omega)$ is the source correlation matrix, defined by

$$W^S_{ij}(\mathbf{r},\mathbf{r}';\omega)\,\delta(\omega-\omega')=\langle J^*_i(\mathbf{r},\omega)J_j(\mathbf{r}',\omega')\rangle, \tag{3}$$

where the angular brackets denote ensemble averages. In order to focus on the contribution that arises due to spatial correlations we assume that the $\mathbf{r}_a$ dependence factorizes, that is,

$$W^S_{ij}(\mathbf{r}_a,\mathbf{\Delta},\omega)=\sum_l j_{il}(\mathbf{r}_a)G_{lj}(\mathbf{\Delta},\omega). \tag{4}$$

This equation defines the two matrices $j_{ij}(\mathbf{r}_a)$ and $G_{ij}(\mathbf{\Delta},\omega)$. We also assume that $G_{ij}(\mathbf{\Delta}=0,\omega)=N\mathcal{S}(\omega)\delta_{ij}$ where N is a normalization factor and and $\mathcal{S}(\omega)$ is the spectrum of light emitted by any point on the source. By substituting this in Eq. (2) we find that

$$J_{ij}(\mathbf{R},\omega)=Z(\omega)\sum_{l,n,m}\xi_{il}\frac{J^0_{ln}\tilde{G}_{nm}(\mathbf{k},\omega)}{R^2}\xi_{mj}, \tag{5}$$

where

$$J^0_{ln}=\int d^3r_a j_{ln}(\mathbf{r}_a) \tag{6}$$

and

$$\tilde{G}_{nm}(\mathbf{k},\omega)=\int d^3\Delta G_{nm}(\mathbf{\Delta},\omega)e^{i\mathbf{k}\cdot\mathbf{\Delta}}, \tag{7}$$

with $\mathbf{k}=k\hat{\mathbf{R}}$. It is clear that in general in the far zone the polarization acquires a nontrivial dependence on frequency ω as well as the angular position of the observation point $\hat{R}$. In Ref. [32] it was shown that the polarization does not have any spectral dependence if and only if $G_{lm}(\mathbf{\Delta},\omega)$ satisfies either of the following conditions:

$$G_{lm}(\mathbf{\Delta},\omega)=h(\omega)G_{lm}(\omega\mathbf{\Delta}), \tag{8}$$

or

$$G_{lm}(\mathbf{\Delta},\omega)=\delta_{lm}H(\mathbf{\Delta},\omega). \tag{9}$$

In the present paper we are interested in the angular, i.e., $\hat{R}$, dependence of the polarization observed in the far zone. We see from Eq. (7) that the polarization in the far zone is independent of $\hat{R}$ if and only if $\tilde{G}_{nm}$ can be written as

$$\tilde{G}_{nm}(\mathbf{k},\omega)=G^{(1)}_{nm}(\omega)\tilde{G}^{(2)}(\mathbf{k},\omega), \tag{10}$$

where $\tilde{G}^{(2)}(\mathbf{k},\omega)$ is some function of $\mathbf{k}$ and ω and $G^{(1)}_{nm}(\omega)$ is a matrix independent of $\hat{R}$. Taking the inverse Fourier transform of $\tilde{G}_{nm}(\mathbf{k},\omega)$ we find that this translates into the following condition:

$$G_{nm}(\mathbf{\Delta},\omega)=G^{(1)}_{nm}(\omega)G^{(2)}(\mathbf{\Delta},\omega), \tag{11}$$

where $G^{(2)}(\mathbf{\Delta},\omega)$ is the inverse Fourier transform of $\tilde{G}^{(2)}(\mathbf{k},\omega)$.

III. POLARIZED RADIATION FROM TWO MONOCHROMATIC POINT SOURCES

We next consider some simple examples in order to illustrate the effect. Since we are primarily interested in investigating the angular dependence of polarization we consider only monochromatic sources. We first consider two polarized point sources P_1 and P_2 which are located along the z axis at a distance $2z$ apart, in analogy to a similar situation considered by Wolf [2] for the unpolarized case. The electric field at the point Q located at large distances R_1 and R_2 from these point sources can be written as

$$\mathbf{E}=\mathbf{e}(\mathbf{r}_1,\omega)\frac{e^{ikR_1}}{R_1}+\mathbf{e}(\mathbf{r}_2,\omega)\frac{e^{ikR_2}}{R_2}. \tag{12}$$

Here $\mathbf{r}_1$ and $\mathbf{r}_2$ are the position vectors of the points P_1 and P_2 and $\mathbf{e}(\mathbf{r}_1,\omega)$ and $\mathbf{e}(\mathbf{r}_2,\omega)$ characterize the strengths of the two sources. The explicit form of $\mathbf{e}(\mathbf{r}_1,\omega)$ and $\mathbf{e}(\mathbf{r}_2,\omega)$ for some simple physically motivated systems will be given below. We calculate the coherency matrix for this electric field at some point Q (Fig. 2) in the far zone.

In order to illustrate the contribution of the cross correlation term we assume that the two sources are simple dipoles $\mathbf{p}_1$ and $\mathbf{p}_2$ located at z and $-z$, respectively, and oriented such that their polar angles $\theta_1=\theta_2=\theta_p$ and the azimuthal angles $\phi_1=-\phi_2=\pi/2$. We assume that θ_p lies between 0 and $\pi/2$. The strength of the dipoles is p_0 and they radiate at frequency ω. We compute the electric field at point Q located at coordinates (R,θ,ϕ), as shown in Fig. 2, such that $R\gg z$. The electric field in the far zone is given by Eq. (12) where the unit vectors $\hat{\mathbf{e}}(\mathbf{r}_1)$ and $\hat{\mathbf{e}}(\mathbf{r}_2)$ in the directions of $\mathbf{e}(\mathbf{r}_1,\omega)$ and $\mathbf{e}(\mathbf{r}_2,\omega)$, respectively, are given by $\hat{\mathbf{e}}(\mathbf{r}_1)=\hat{\mathbf{p}}_1\cdot\hat{\mathbf{R}}\hat{\mathbf{R}}-\hat{\mathbf{p}}_1$ and $\hat{\mathbf{e}}(\mathbf{r}_2)=\hat{\mathbf{p}}_2\cdot\hat{\mathbf{R}}\hat{\mathbf{R}}-\hat{\mathbf{p}}_2$. We also assume that in the denominators of the two terms on the right hand side

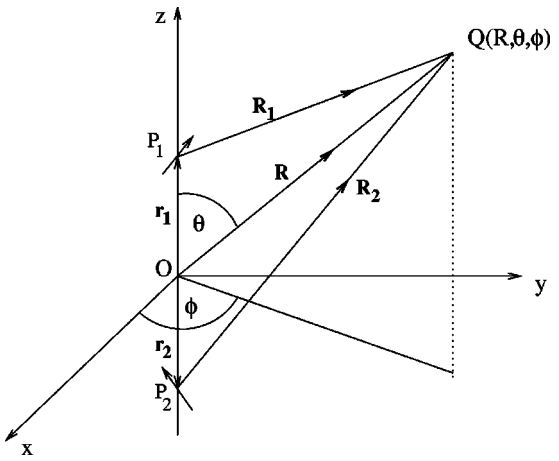

FIG. 2. Schematic illustration of two polarized monochromatic point sources P_1 and P_2 located at $\mathbf{r}_1$ and $\mathbf{r}_2$, respectively. The observation point Q is at a distance R which is much larger than the spatial extent of the source.

of Eq. (12) R_1 and R_2 can be replaced by $R_1=R_2=R$, which is a reasonable approximation in the far zone. Hence, up to an overall factor that is irrelevant for our purpose, the field in the far zone is given by the addition of two vectors $\hat{\mathbf{p}}_1\cdot\hat{\mathbf{R}}\hat{\mathbf{R}}-\hat{\mathbf{p}}_1$ and $\hat{\mathbf{p}}_2\cdot\hat{\mathbf{R}}\hat{\mathbf{R}}-\hat{\mathbf{p}}_2$ with phase difference of $2\omega z\cos\theta/c$. The vector $\hat{\mathbf{p}}\cdot\hat{\mathbf{R}}\hat{\mathbf{R}}-\hat{\mathbf{p}}$ at any point (R,θ,ϕ) is of course simply the projection of the polarization vector $\hat{\mathbf{p}}$ on the plane perpendicular to $\hat{\mathbf{R}}$ at that point. We keep only the leading order terms in z/R in computing the total electric field.

The observed polarization is obtained by calculating the coherency matrix, given by

$$J=\begin{pmatrix}\langle E_\theta E_\theta^*\rangle & \langle E_\theta E_\phi^*\rangle\\ \langle E_\phi E_\theta^*\rangle & \langle E_\phi E_\phi^*\rangle\end{pmatrix}. \tag{13}$$

The state of polarization can be uniquely specified by the Stokes parameters or equivalently the Poincaré sphere variables [33]. The Stokes parameters are obtained in terms of the elements of the coherency matrix as $S_0=J_{11}+J_{22}$, $S_1=J_{11}-J_{22}$, $S_2=J_{12}+J_{21}$, $S_3=i(J_{21}-J_{12})$. The parameter S_0 is proportional to the intensity of the beam. The Poincaré sphere is charted by the angular variables 2χ and 2ψ, which can be expressed as

$$S_1=S_0\cos(2\chi)\cos(2\psi),\quad S_2=S_0\cos(2\chi)\sin(2\psi),$$

$$S_3=S_0\sin(2\chi). \tag{14}$$

The angle χ $(-\pi/4\leq\chi\leq\pi/4)$ measures the ellipticity of the state of polarization and ψ $(0\leq\psi<\pi)$ measures the alignment of the linear polarization. For example, $\chi=0$ represents pure linear polarization and $\chi=\pi/4$ pure right circular polarization.

The Stokes parameters at the observation point Q for the two-dipole source are given by

$$S_0=\left(\frac{\omega^2 p_0}{c^2R}\right)^2\{4\cos^2[\omega z(\cos\theta)/c]\cos^2\theta_p\sin^2\theta$$
$$+4\sin^2[\omega z(\cos\theta)/c]\sin^2\theta_p(\cos^2\theta\sin^2\phi+\cos^2\phi)\},$$

$$S_1=\left(\frac{\omega^2 p_0}{c^2R}\right)^2\{4\cos^2[\omega z\,(\cos\theta)/c]\cos^2\theta_p\sin^2\theta$$
$$+4\sin^2[\omega z(\cos\theta)/c]\sin^2\theta_p(\cos^2\theta\sin^2\phi-\cos^2\phi)\},$$

$$S_2=\left(\frac{\omega^2 p_0}{c^2R}\right)^2 8\sin^2[\omega z(\cos\theta)/c]\sin^2\theta_p\cos\theta\sin\phi\cos\phi,$$

$$S_3=\left(\frac{\omega^2 p_0}{c^2R}\right)^2 8\cos[\omega z(\cos\theta)/c]\sin[\omega z(\cos\theta)/c]$$
$$\times\cos\theta_p\sin\theta_p\sin\theta\cos\phi. \tag{15}$$

The resulting polarization in the far zone is quite interesting. At $\sin\phi=0$, $\theta=\pi/2$ the wave is linearly polarized ($\chi=0$) with $\psi=0$. As θ decreases from $\pi/2$ to 0, $\chi>0$ and the wave has general elliptical polarization with $\psi=0$. At a certain value of the polar angle $\theta=\theta_t$ the wave is purely right circularly polarized. As θ crosses θ_t, the linearly polarized component jumps from 0 to $\pi/2$, i.e., 2ψ changes from 0 to π. The value of the polar angle θ_t at which the transition occurs is determined by

$$\tan[\omega z(\cos\theta_t)/c]=\pm\sin\theta_t/\tan\theta_p. \tag{16}$$

From this equation we see that, as $z\to 0$, the transition angle θ_t is close to zero for a wide range of values of θ_p. Only when $\theta_p\to\pi/2$ can a solution with θ_t significantly different from 0 be found. In general, however, we can find a solution with any value of θ_t by appropriately adjusting z and θ_p. If the value of $(\omega z/c)$ is large enough we also find multiple values of θ_t that satisfy Eq. (16). It is clear that even if θ_p is small, which physically means that both the dipole orientations make very small angles with the z axis, by suitably choosing $\omega z/c$ large enough we can get multiple polarization flips even at polar angles of the observation point close to $\pi/2$. For $\sin\phi>0$, we find qualitatively similar results, except that now the linear polarization angle 2ψ increases smoothly from 0 as θ goes from $\pi/2$ to 0. Furthermore, the state of polarization never becomes purely circular, i.e., the angle 2χ is never equal to $\pi/2$ although it does achieve a maximum at θ close to the transition angle θ_t given by Eq. (5).

Experimentally the situation we have discussed above is analogous to the standard two-slit interference experiment except that we are considering the detailed polarization structure of the interfering waves. We can set up an experiment to study the polarization interference effects by illuminating the two slits with a coherent circularly polarized beam. We place a polarizer in front of each slit in order to get the desired linear polarization. The two slits then act as secondary sources of electromagnetic waves. Referring again to Fig. 2 we assume that the screen containing the two slits lies in the z-y plane. The polarizers are aligned such that they are also

parallel to this plane. For simplicity we assume that the observation point Q lies in the x-z plane, i.e., $\phi=0$. The resulting interference pattern can be computed by using the vector diffraction theory [34]. The electric field due to a single slit centered at $\mathbf{r}_1$ is given by

$$\mathbf{E}_1(\mathbf{R})=\frac{1}{2\pi}\boldsymbol{\nabla}\times\int[\hat{\mathbf{n}}\times\mathbf{E}(\mathbf{r}_1)]\frac{e^{ikR_1}}{R_1}da_1. \tag{17}$$

Here $\mathbf{E}_1(\mathbf{R})$ is the diffracted wave, $\mathbf{E}(\mathbf{r}_1)$ is the electric field at the position of the slit, $\hat{\mathbf{n}}$ is the unit vector perpendicular to the slit, and the integration is over the area of the opening. We assume that the electric field vector $\mathbf{E}$ is constant over the slit and then we find that

$$\mathbf{E}_1(\mathbf{R})=C\frac{e^{ikR}}{R}(\hat{\mathbf{n}}\hat{\mathbf{R}}\cdot\hat{\mathbf{p}}_1-\hat{\mathbf{p}}_1\hat{\mathbf{R}}\cdot\hat{\mathbf{n}}), \tag{18}$$

where C is a constant which will not play any role in our analysis, $\hat{\mathbf{p}}_1$ is a unit vector in the direction of the electric field $\mathbf{E}(\mathbf{r}_1)$, and we have ignored higher order terms in z/R. The total electric field $\mathbf{E}_T$ at the point Q is obtained by adding the contributions from the two slits. Let Δ be the angle between the orientations of the linear polarization at the two slits. We take the z axis to be aligned symmetrically between these two polarization vectors and thus $\theta_p=\Delta/2$. The resulting Stokes parameters are given by

$$\begin{aligned}
S_0&=\left(\frac{2C}{R}\right)^2\{\cos^2[\omega z(\cos\theta)/c]\cos^2\theta_p\\
&\quad+\sin^2[\omega z(\cos\theta)/c]\sin^2\theta_p\sin^2\theta\},\\
S_1&=\left(\frac{2C}{R}\right)^2\{\cos^2[\omega z(\cos\theta)/c]\cos^2\theta_p\\
&\quad-\sin^2[\omega z(\cos\theta)/c]\sin^2\theta_p\sin^2\theta\},\\
S_2&=0\\
S_3&=\left(\frac{2C}{R}\right)^2 2\cos[\omega z(\cos\theta)/c]\sin[\omega z(\cos\theta)/c]\\
&\quad\times\cos\theta_p\sin\theta_p\sin\theta.
\end{aligned} \tag{19}$$

The transition angle in this case is given by the equation

$$\tan[\omega z(\cos\theta_t)/c]=\pm\frac{1}{\sin\theta_t\tan\theta_p}. \tag{20}$$

It is well known that the interference intensity pattern depends on the state of polarization of the two sources. We find that the polarization pattern also oscillates in a manner analogous to the oscillations in intensity. We consider $\omega z/c\gg1$, in which case we find that there exist a large number of intensity maxima. The positions of these maxima (and minima) as a function of the polar angle θ are obtained by setting the derivative of S_0 with respect to θ equal to zero. If we consider the interference pattern close to $\theta=\pi/2$ then we find that the maxima and minima occur at the positions

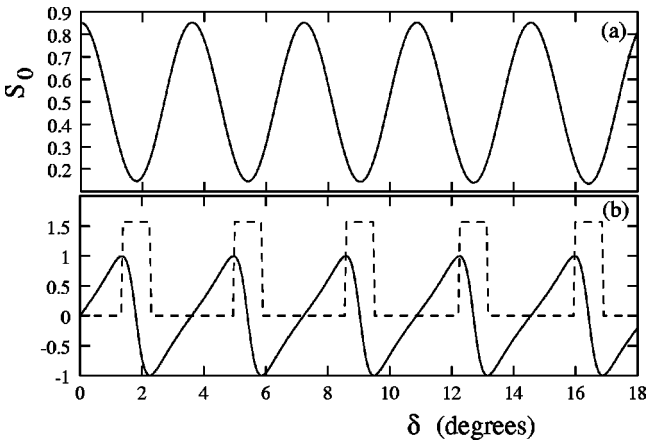

FIG. 3. (a) The intensity S_0 (in arbitrary units) due to interference of electromagnetic radiation from two slits is plotted as a function of the angle $\delta=90-\theta$ (in degrees) with respect to the unit normal to the screen containing the slits. Here θ is the polar angle as defined in text. The angular dependences of $\sin 2\chi$ (solid line), which is a measure of the ellipticity of the state of polarization, and the linear polarization angle ψ (dashed line) are shown in (b). The parameters used for this plot are $\omega z/c=50$ and $\Delta=\pi/4$, where Δ is the angle between the orientations of linear polarization at the two slits.

$$\omega z(\cos\theta)/c\approx n\pi \quad\text{or}\quad (n+1/2)\pi, \tag{21}$$

as we expect. For a wide range of values of the parameter θ_p we find that $\omega z(\cos\theta)/c\approx n\pi$ gives the position of the maxima. However if $\cos^2\theta_p<\sin^2\theta_p\sin^2\theta$, then $n\pi$ actually gives a minimum. The polarization pattern also fluctuates in the same manner. The angle θ where the polarization is completely linearly polarized, i.e., $S_3=0$, is again given by Eq. (21). We further find that for the case of the two-slit experiment the polarization at the minima is orthogonal to that at the maxima.

In order to illustrate this point we compare in Fig. 3 the intensity pattern S_0 with the state of circular polarization. We set the parameter $\omega z/c=50$, which implies that the distance between the two slits is large compared to the wavelength of light. In this case we expect a large number of interference fringes, which are shown in Fig. 3(a) as a function of the angle $\delta=\pi/2-\theta$ (in radians) between the unit normal to the screen containing the slits and the direction of observation. The pattern of fringes of course depends on the state of polarization of the two sources. The electromagnetic wave at the two slits is assumed to be linearly polarized with the angle Δ between the polarization at the two slits equal to $\pi/4$. Hence the polarization at the two slits has the polar angle $\theta_p=\pi/8$. In Fig. 3(b) we plot $\sin 2\chi$, which illustrates the state of circular polarization with $\sin 2\chi=1$ representing pure right circular polarization. The state of circular polarization also oscillates such that we find pure linear polarization at the location of both maxima and minima. However, the orientation of linear polarization at maxima is at right angles to the polarization at minima. This effect can be measured experimentally by performing the standard two-slit interference experiment using polarized light. We assume that

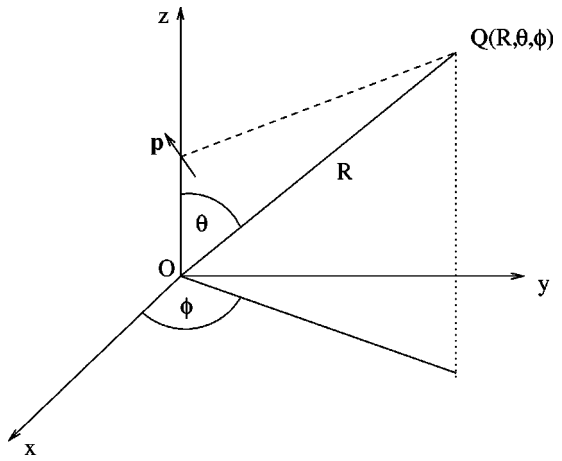

FIG. 4. The correlated source consisting of an array of dipoles aligned along the z axis. The observation point Q is at a distance R which is much larger than the spatial extent of the source.

the two slits are illuminated by a circularly polarized monochromatic light that has perfect spatial correlation. The state of polarization at the two slits can be changed to linear polarization at desired orientations using polarizers. The polarization can then be measured at a faraway point at different angular positions.

IV. CONTINUOUS SPATIALLY CORRELATED SOURCES

We next discuss the more general case of continuous spatially correlated sources. In the case of a primary source the electric field in the radiation zone is given by Eq. (1). We will again specialize only to monochromatic sources and assume perfect coherence over the entire source so that the degree of polarization is equal to unity. We expect that the polarization will display a nontrivial angular dependence in the far zone and illustrate this by taking some simple examples of one-dimensional sources.

A. A one-dimensional spatially correlated source

A simple continuous model of a monochromatic spatially correlated source can be constructed by arranging a series of dipoles along a line with their orientations correlated with the position of the source. The dipoles will be taken to be aligned along the z axis and distributed as a Gaussian exp $[-z^2/2\sigma^2]$. The orientation of the dipole is characterized by the polar coordinates θ_p, ϕ_p, which are also assumed to be correlated with the position z. A simple correlated ansatz is given by

$$\frac{\exp[\alpha\cos\theta_p+\beta z\sin\phi_p]}{N_1(\alpha)N_2(\beta z)}, \tag{22}$$

where α and β are parameters, $N_1(\alpha)=\pi I_0(\alpha)$ and $N_2(\beta z)=2\pi I_0(\beta z)$ are normalization factors, and I_0 is the Bessel function. The basic distribution function $\exp(\alpha\cos[\theta-\theta_0)]$ used in the above ansatz is the well known von Mises distribution which for circular data is in many ways the analog of a Gaussian distribution for linear data [35–37]. For $\alpha>0$ this function peaks at $\theta=\theta_0$. Making a Taylor expansion close to its peak, we find a Gaussian distribution to leading power in $\theta-\theta_0$. The maximum likelihood estimators for the mean angle θ_0 and the width parameter α are given by $\langle\sin(\theta-\theta_0)\rangle=0$ and $\langle\cos(\theta-\theta_0)\rangle=d\ln[I_0(\alpha)]/d\alpha$, respectively. In prescribing the ansatz given in Eq. (22) we have assumed that the polar angle θ_p of the dipole orientation is uncorrelated with z and the distribution is peaked at $\theta_p=0$ (π) for $\alpha>0$ (<0). The azimuthal angle ϕ_p is correlated with z such that for $\beta>0$ and $z>0(<0)$ the distribution peaks at $\phi_p=\pi/2(3\pi/2)$.

We next calculate the electric field at very large distance from such a correlated source. The observation point Q is located at the position (R,θ,ϕ) (Fig. 4), measured in terms of the spherical polar coordinates, and we assume that the spatial extent of the source $\sigma\ll R$. The electric field from such a correlated source at large distances is given by

$$\mathbf{E}=-\frac{\omega^2}{c^2R}p_0e^{i(-\omega t+R\omega/c)}\int_{-\infty}^{\infty}dz\,\exp(-z^2/2\sigma^2)$$
$$\times\int_0^{\pi}d\theta_p\int_0^{2\pi}d\phi_p\times\frac{\exp(\alpha\cos\theta_p+\beta z\sin\phi_p)}{2\pi^2I_0(\alpha)I_0(\beta z)}$$
$$\times\exp(i\omega z\hat{\mathbf{R}}\cdot\hat{\mathbf{z}}/c)(\hat{\mathbf{p}}\cdot\hat{\mathbf{R}}\hat{\mathbf{R}}-\hat{\mathbf{p}}), \tag{23}$$

where $\hat{\mathbf{p}}$ is a unit vector parallel to the dipole axis, p_0 is the strength of the dipole, ω is the frequency of light, and I_0 denotes the Bessel function. Since we are interested in the radiation zone we have dropped all terms higher order in z/R. The resulting field is of course transverse, i.e., $\mathbf{E}\cdot\hat{\mathbf{R}}=0$. We have also assumed that all the dipoles radiate at the same frequency and are in phase. The spatial correlation of the source is measured by the parameter β.

It is convenient to define scaled variable $\bar{z}=z/\sigma$, $\bar{\lambda}=\lambda/\sigma$ where $\lambda=2\pi\omega/c$ is the wavelength, and $\bar{\beta}=\beta\sigma$. The integrations over θ_p and ϕ_p can be performed analytically. We numerically integrate over z for various values of position of the observation point, different values of the parameter α that determines the width of the distribution of θ_p, and different values of the correlation parameter β.

We first study the situation where $\bar{\beta}>0$ and $\alpha>0$. The results for several values of (θ,ϕ) are given in Figs. 5 and 6 which show plots of the Poincaré sphere variables 2χ and 2ψ. The scaled wavelength $\bar{\lambda}=\lambda/\sigma$ of the emitted radiation is taken to be equal to π, i.e., the effective size of the source σ is of the order of the wavelength λ. The results show several interesting aspects. The ellipticity of the state of polarization shows significant dependence on the position of the observer. The angle $\chi=0$, i.e., the beam has pure linear polarization, for the polar angle $\cos\theta=0,1$ for all values of the azimuthal angle ϕ. It deviates significantly from 0 as $\cos\theta$ varies from 0 to 1. For $\sin\phi=0$, $2\chi=\pi/2$ at some critical value θ_t as $\cos\theta$ varies between 0 and $\pi/2$, i.e., the state of polarization is purely right circular at $\theta=\theta_t$. For $\sin\phi>0$, 2χ also deviates significantly from 0 and displays a

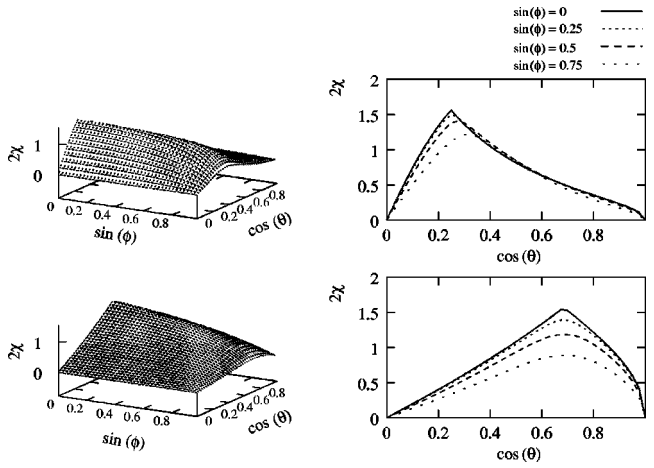

FIG. 5. The polar angle on the Poincaré sphere, 2χ, which is a measure of the eccentricity of the ellipse traced by the electric field vector. For pure linear polarization $2\chi=0$ and for pure right circular polarization $2\chi=\pi/2$. The 3D plots show 2χ as a function of $\cos\theta$ and $\sin\psi$ where θ and ϕ are the polar and azimuthal angles of the point of observation. The 2D plots on the right show the corresponding slices of the 3D plots for different values of $\sin\phi$. The upper and lower plots correspond to $\bar{\beta}=1$, $\alpha=0.25$ and $\bar{\beta}=\alpha=1$, respectively.

peak at some value of θ. The precise position of the peak is determined by the values of the correlation parameters α and $\bar{\beta}$.

The alignment of linear polarization also shows some very interesting aspects. For $\sin\phi=0$, we find that ψ is either 0 or π depending on the value of θ. The transition occurs at the same critical value of θ where the angle χ shows a peak. The state of polarization is purely linear with the electric field along $\hat{\theta}$ for $\cos\theta=0$ and then acquires a circular component for increasing values of $\cos\theta$. At the transition point $\theta=\theta_t$, the polarization is purely circular. With further increase in the value of θ the state of polarization is elliptical with the linearly polarized component aligned along $\hat{\phi}$. The transition point is clearly determined by the conditions $S_1=J_{11}-J_{22}=0$ and $S_2=J_{12}+J_{21}=0$.

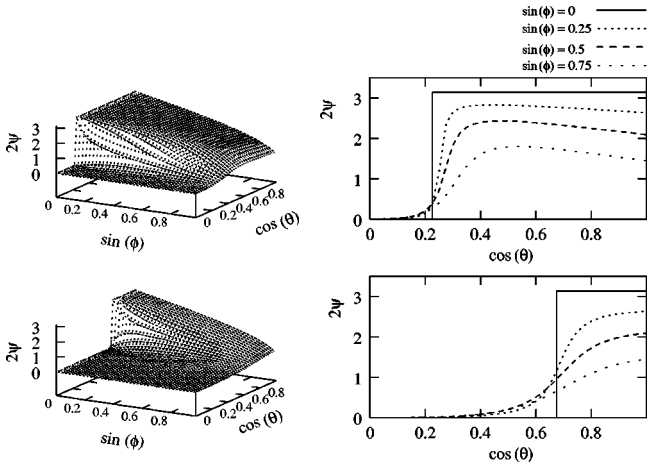

FIG. 6. The azimuthal angle on the Poincaré sphere, 2ψ. This measures the orientation of the linearly polarized component of the wave. The 3D plots show 2ψ as a function of $\cos\theta$ and $\sin\psi$ where θ and ϕ are the polar and azimuthal angles of the point of observation. The 2D plots on the right show the corresponding slices of the 3D plots for different values of $\sin\phi$. The upper and lower plots correspond to $\bar{\beta}=1$, $\alpha=0.25$, and $\bar{\beta}=\alpha=1$ respectively.

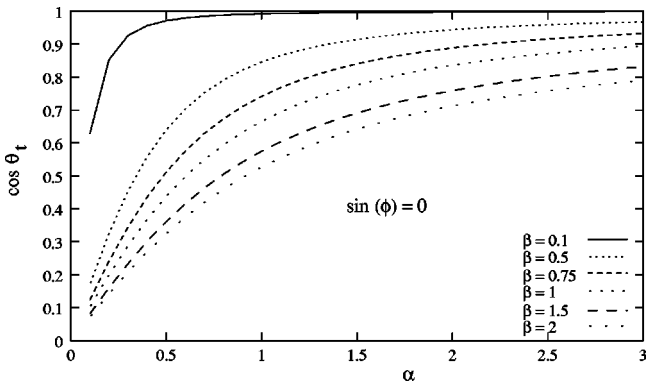

FIG. 7. The critical value of the polar angle θ at which the state of linear polarization shows a sudden transition for $\sin\phi=0$ as a function of the parameters α and β that specify the distribution of the dipole orientations. For any given values of the parameters α and β, the electric field is parallel ($\psi=0$) to the z axis if the cosine of the observation polar angle, $\cos\theta$, is less than $\cos\theta_t$. On the other hand the electric field is perpendicular to the z axis if $\cos\theta$ is greater than $\cos\theta_t$.

For other values of $\sin\phi$ we find that $\psi=0$ for $\cos\theta=0$ and then deviates significantly from 0 as θ approaches θ_t, finally leveling off as $\cos\theta$ approaches 1. The final value of ψ at $\cos\theta=1$ depends on the correlation parameters and $\sin\phi$ but for a wide range of parameters $2\psi>\pi/2$. We see from Fig. 7 that the linear polarization from sources of this type shows a striking characteristic, i.e., that the polarization angle ψ is close to either 0 or $\pi/2$ depending on the angle at which it is viewed.

For $\sin\phi<0$ the Poincaré sphere polar angle 2χ is the same as for $\sin\phi>0$; however, the orientation of the linear polarization 2ψ lies between π and 2π, i.e., in the third and fourth quadrants of the equatorial plane on the Poincaré sphere. For a particular value of ϕ the azimuthal angle $\psi(\phi)=-\psi(-\phi)$.

If we change the sign of α we do not find any change in linear polarization angle ψ; however, the value of χ changes sign, i.e., the state of polarization changes from right elliptical to left elliptical. The change in sign of $\bar{\beta}$ also leaves ψ unchanged while changing the sign of χ. Changing the signs of both α and $\bar{\beta}$ produces no change at all.

In the case of the limiting situation where $\bar{\beta}=0$ we find, as expected, that the linear polarization is independent of the angular position, i.e., $\chi=0$ and $\psi=0$. This is true for any value of the parameter α, which determines the polar distribution of the dipole orientations. Hence we see that the effect disappears if either the effective size of the source $\sigma=0$ or the correlation parameter $\beta=0$. The effect also disappears in the limit $\alpha\to\infty$. In this limit the distribution of θ_p is simply a δ function peaked at 0 and hence our model reduces to a

series of dipoles aligned along the z axis, which cannot give rise to any nontrivial structure. In the numerical calculations above we have taken the effective size of the source σ of the order of the wavelength λ. If the size $\sigma \ll \lambda$, the effect is again negligible since the phase factor $\omega z \hat{R} \cdot \hat{z}/c$ in Eq. (23) is much smaller than 1 in this case.

Hence we find that in order to obtain a nontrivial angular dependence of the state of polarization the size of the source, assumed to be coherent, has to be of the order of or larger than the wavelength.

B. Transition angle

From our results we see that there exists a critical value of the polar angle θ at which the state of linear polarization changes very rapidly. This is particularly true if we set $\sin\phi = 0$, where we find that the orientation of linear polarization ψ suddenly jumps from 0 (or π) to $\pi/2$ at some critical value of the polar angle $\theta = \theta_t$. We study this case in a little more detail. The θ and ϕ components of the total electric field are given by

$$E_\theta = -\frac{\omega^2 p_0}{c^2 R} e^{-i\omega(t-R/c)} \sqrt{2\sigma^2\pi}\, e^{-\sigma^2\omega^2\cos^2\theta/2c^2} \frac{I_1(\alpha)}{I_0(\alpha)} \sin\theta$$

$$E_\phi = i\frac{\omega^2 p_0}{c^2 R} e^{-i\omega(t-R/c)} \frac{2\sinh\alpha}{\alpha\pi I_0(\alpha)} A,$$

where

$$A = \int_{-\infty}^{\infty} dz e^{-z^2/2\sigma^2} \sin[\omega z \cos\theta/c] \frac{I_1(\beta z)}{I_0(\beta z)}.$$

In this case the Stokes parameter $S_2 = 0$. For $\beta \geqslant (<)\ 0$, $S_3 \geqslant (<)\ 0$ and hence $\chi \geqslant (<)\ 0$. The point where the polarization angle 2ψ jumps from 0 to π is determined by the condition $S_1 = 0$. This is clearly also the point where $2\chi = \pm\pi/2$. Explicitly, the condition to determine the critical value θ_t is

$$A^2 = \sigma^2\pi^3\alpha^2 e^{-\sigma^2\omega^2\cos^2\theta_t/c^2} \sin^2\theta_t \frac{I_1(\alpha)^2}{2\sinh^2\alpha}. \qquad (24)$$

This can be used to determine θ_t as a function of α and β. The result for $\cos\theta_t$ as a function of α is plotted in Fig. 7 for several different values of β. For any fixed value of the parameter β, the transition angle θ_t decreases from $\pi/2$ to 0 as α goes from zero to infinity. This is expected since as α becomes large the polar angle distribution of the dipole orientations, peaked along the z axis, becomes very narrow and hence the resultant electric field is aligned along the z axis for a large range of polar angle θ. Furthermore, we find, as expected, that as β goes to zero the transition angle also tends toward 0.

C. Correlation with intensity in the radiation zone

We next examine how the polarization is correlated with the angular dependence of intensity in the far zone. In the case of two slits we found strong correlation in the sense that the wave was linearly polarized at the positions of the minima and maxima of intensity. In the present case we do not find any such correlation. The intensity profile for this case is plotted in Fig. 8 with the parameters $\bar{\beta} = 1$ and $\alpha = 0.25$. The polarization profile for this choice of parameters is shown in the upper plots in Figs. 5 and 6. It is clear that the positions of the intensity extrema do not correspond to any special points on the polarization profiles. Hence the strong correlation found in the case of two slits is absent in the present case. The condition for intensity extrema, $\partial S_0/\partial\theta = 0$, is clearly distinct from the condition $S_3 = 0$ that requires that the wave is purely linearly polarized. Only in the special case of two slits were these two conditions equivalent.

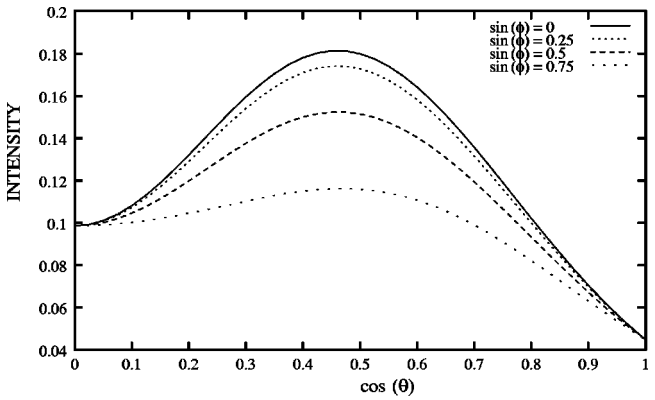

FIG. 8. The intensity profile S_0 (in arbitrary units) in the radiation zone as a function of $\cos\theta$ for different values of $\sin\phi$ for the parameters $\bar{\beta} = 1$, $\alpha = 0.25$.

D. Helical model

We next study an interesting generalization of the model discussed above. Instead of having the peak of the ϕ_p distribution fixed to $-\pi/2$ for $z<0$ and $\pi/2$ for $z>0$ we allow it to rotate in a helix circling around the z axis. In this case we replace the ϕ_p dependence by $\exp[\beta(\phi_p - \xi z)]$. As z goes from negative to positive values, the peak of the distribution rotates clockwise around the z axis forming a helix. The z distribution in Eq. (23) is taken to be uniform, and the source extends from $z = -\sigma$ to $z = \sigma$. We study this in detail by fixing the azimuthal angle of the dipole orientation $\phi_p = \xi z$ and the polar angle θ_p to some constant values, i.e., the ϕ_p and θ_p distributions are both assumed to be δ functions. This allows us to perform the z integration in Eq. (23) analytically. The resulting states of polarization, described by Poincaré sphere angles 2χ and 2ψ, are shown in Figs. 9–12. In this model we can extract a simple rule to determine the transition angle for the special case $\theta_p = \pi/2$ and $\xi = n\pi$ where n is an integer. We set $\sin\phi = 0$ for this calculation since it is only for this value that the polarization becomes purely circular for some value of $\theta = \theta_t$ and the linearly polarized component flips by $\pi/2$ at this point. A straightforward calculation shows that this transition angle θ_t is given by

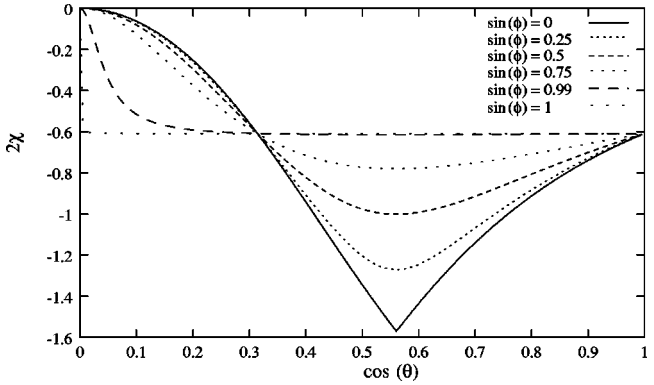

FIG. 9. The polar angle on the Poincaré sphere, 2χ (rad), for the helical model as a function of $\cos\theta$ ($\bar{\lambda}=0.2\pi, \theta_p=\pi/2, \xi=\pi$).

$$\cos^2\theta_t = n\bar{\lambda}/2. \tag{25}$$

Here n represents the number of π radians that are traversed by the tip of the electric field vector along the helical path and $\bar{\lambda}=\lambda/\sigma$ where λ is the wavelength. In order to get at least one transition $\bar{\lambda}<2/n$. In the special case under consideration there is at most one transition. However, in general, the situation is more complicated and for certain values of θ_p and ξ, more than one transition is possible. Some representative examples are shown in Figs. 9–12. In this case also we do not find any direct correlation between the intensity extrema and the polarization profile. For the simple case of $\theta_p=\pi/2$, $\xi=n\pi$, and $\sin\phi=0$, for which the transition angle is given by Eq. (25), we find that the intensity extrema are given by $\cos\theta=m\bar{\lambda}/2$, where m is any integer. Hence it is clear that neither the number nor the positions, of the intensity extrema have any direct correlation with the number and positions of transitions in the polarization profile.

V. DISCUSSION AND CONCLUSIONS

In this paper we have considered spatially correlated monochromatic sources. We find that at large distance the polarization of the wave shows a dramatic dependence on the angular position of the observer. For certain sets of parameters the linearly polarized component shows a sudden jump by $\pi/2$. If the symmetry axis of the source is taken to be the z axis, the polarization shows a sudden transition from parallel to perpendicular to the symmetry axis of the source, as the polar angle is changed from $\pi/2$ to 0. The sources considered in this paper are idealized since we have assumed coherence over the entire source. For small enough sources this may a reasonable approximation. In the case of macroscopic sources, this assumption is in general not applicable. However, in certain situations some aspects of the behavior described in this paper may survive even for these cases. We may consider a macroscopic source consisting of a large number of structures of the type considered in this paper. As long as there is some correlation between the orientation of these structures over large distances we expect that some aspects of the angular dependence of the polarization of the small structures will survive, even if no coherent phase relationship exists over large distances. Hence the ideas discussed in this paper may also find interesting applications to macroscopic and astrophysical sources. An interesting astrophysical example is the synchrotron radiation from magnetized plasma in sources such as pulsars, radio galaxies, and quasars. Large scale spatial correlation may be expected in these cases. It is also well known that the polarization angle

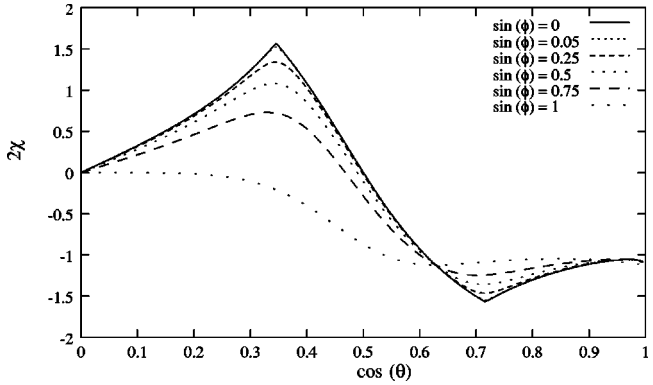

FIG. 11. The polar angle on the Poincare sphere, 2χ (radians) for the helical model as a function of $\cos\theta$ ($\bar{\lambda}=0.4\pi, \theta_p=\pi/4, \xi=\pi$).

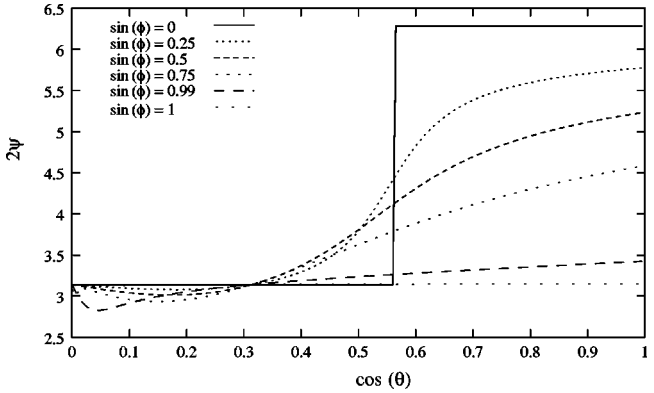

FIG. 10. The azimuthal angle on the Poincaré sphere, 2ψ (radians) for the helical model as a function of $\cos\theta$ ($\bar{\lambda}=0.2\pi, \theta_p=\pi/2, \xi=\pi$).

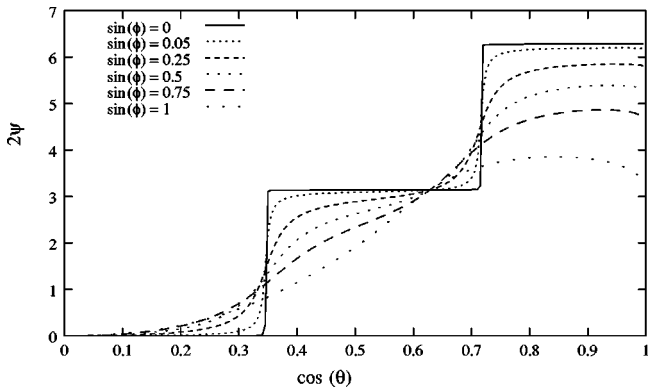

FIG. 12. The azimuthal angle on the Poincaré sphere, 2ψ (rad), for the helical model as a function of $\cos\theta$ ($\bar{\lambda}=0.4\pi, \theta_p=\pi/4, \xi=\pi$).

of radio galaxies and quasars is predominantly observed to be aligned either parallel or perpendicular to the source orientation axis [38]. This difference has generally been attributed to the existence of different physical mechanisms for the generation of radio waves in these sources. Our study, however, indicates that this difference in observed polarization angle could also arise simply due to different angles of observation. Hence orientation effects must be considered before assuming different physical mechanisms for differences in the observed polarizations of these sources.

ACKNOWLEDGMENTS

We thank John Ralston, N. Rathnashree, and Harshawardhan Wanare for very useful discussions.

[1] E. Wolf, Phys. Rev. Lett. **56**, 1370 (1986).
[2] E. Wolf, Opt. Commun. **62**, 12 (1987).
[3] E. Wolf, Nature (London) **326**, 363 (1987).
[4] D. Faklis and G.M. Morris, Opt. Lett. **13**, 4 (1988); J. Mod. Opt. **39**, 941 (1992).
[5] F. Gori, G. Guattari, C. Palma, and G. Padovani, Opt. Commun. **67**, 1 (1988).
[6] G. Indebetouw, J. Mod. Opt. **36**, 251 (1989).
[7] For a review, see E. Wolf and D.F.V. James, Rep. Prog. Phys. **59**, 771 (1996).
[8] J. Rai, S. Rai, and S. Chopra, Phys. Rev. A **47**, 4400 (1993).
[9] S. Chopra, S.K.P. Bhat, J. Joseph, S. Rai, and J. Rai, Opt. Commun. **109**, 205 (1994).
[10] D.F.V. James, H.C. Kandpal, and E. Wolf, Astrophys. J. **445**, 406 (1995).
[11] H.C. Kandpal, K. Saxena, D.S. Mehta, J.S. Vaishya, and K.C. Joshi, J. Mod. Opt. **42**, 447 (1995).
[12] S. Vicalvi, G. Shirripa Spagnolo, and M. Santarsiero, Opt. Commun. **130**, 241 (1996).
[13] E. Wolf, T. Shirai, H. Chen, and W. Wang, J. Mod. Opt. **44**, 1345 (1997).
[14] T. Shirai, E. Wolf, H. Chen, and W. Wang, J. Mod. Opt. **45**, 799 (1998).
[15] E. Wolf, J.T. Foley, and F. Gori, J. Opt. Soc. Am. A **6**, 1142 (1989); **7**, 173(E) (1990).
[16] T. Shirai and T. Asakura, J. Opt. Soc. Am. **12**, 1354 (1995).
[17] T. Shirai and T. Asakura, Opt. Commun. **123**, 234 (1996).
[18] T.A. Leskova, A.A. Maradudin, A.V. Shchegrov, and E.R. Mendez, Phys. Rev. Lett. **79**, 1010 (1997).
[19] A. Dogriu and E. Wolf, Opt. Lett. **23**, 1340 (1998).
[20] E. Wolf, Phys. Rev. Lett. **63**, 2220 (1989).
[21] J.T. Foley and E. Wolf, Phys. Rev. A **40**, 588 (1989).
[22] D.F.V. James, M.P. Savedoff, and E. Wolf, Astrophys. J. **359**, 67 (1990).
[23] D.F.V. James and E. Wolf, Phys. Lett. A **146**, 167 (1990).
[24] D.F.V. James and E. Wolf, Phys. Lett. A **188**, 239 (1994).
[25] A.K. Jaiswal, G.P. Agarwal, and C.L. Mehta, Nuovo Cimento Soc. Ital. Fis., B **15**, 295 (1973).
[26] D.F.V. James, J. Opt. Soc. Am. A **11**, 1641 (1994); Opt. Commun. **109**, 209 (1994).
[27] F. Gori, M. Santarsiero, R. Borghi, and G. Piquero, Opt. Lett. **25**, 1291 (2000).
[28] F. Gori, M. Santarsiero, R. Borghi, and G. Guattari, Opt. Commun. **163**, 159 (1999).
[29] F. Gori, M. Santarsiero, S. Vicalvi, R. Borghi, and G. Guattari, J. Opt. A, Pure Appl. Opt. **7**, 941 (1998).
[30] G.P. Agrawal and E. Wolf, J. Opt. Soc. Am. A **17**, 2019 (2000).
[31] G. Gbur and D.F.V. James, J. Mod. Opt. **47**, 1171 (2000).
[32] K. Bhuvalka and P. Jain, Phys. Rev. E **64**, 036607 (2001).
[33] M. Born and E. Wolf, *Principles of Optics* (Pergamon Press, Oxford, 1980).
[34] J. D. Jackson, *Classical Electrodynamics* (John Wiley & Sons, New York, 1998).
[35] K. V. Mardia, *Statistics of Directional Data* (Academic Press, London, 1972).
[36] E. Batschelet, *Circular Statistics in Biology* (Academic Press, London, 1981).
[37] N. I. Fisher, *Statistics of Circular Data* (Cambridge University Press, Cambridge, 1993).
[38] J.N. Clark *et al.*, Mon. Not. R. Astron. Soc. **190**, 205 (1980).